
Monograph:
Peyton-Jones, J.C. and Billings, S.A. (1990) Describing Functions Volterra Series, and the Analysis of Nonlinear Systems in the Frequency Domain. Research Report. Acse Report 396 . Dept of Automatic Control and System Engineering. University of Sheffield

---

DESCRIBING FUNCTIONS, VOLTERRA SERIES, AND THE ANALYSIS OF NONLINEAR SYSTEMS IN THE FREQUENCY DOMAIN

J.C. Peyton Jones.
S.A. Billings,

Department of Control Engineering
University of Sheffield
Mappin Street
Sheffield S1 3JD
U.K.

Research Report No. 396

June 1990

June 18, 1990

DESCRIBING FUNCTIONS, VOLTERRA SERIES, AND THE ANALYSIS OF NONLINEAR SYSTEMS IN THE FREQUENCY DOMAIN

J.C. Peyton Jones, S.A. Billings.

Dept. Control Engineering, University of Sheffield, Mappin Street, Sheffield S1 3JD.

Abstract: A relationship between the higher order frequency response functions of the Volterra series model, and the well known describing function representation for nonlinear systems is derived. It is shown that a large class of generalised describing functions can be derived from the Volterra model and that this approach removes the restriction to specific inputs. The concept of a worst case transfer function is introduced, and examples are included to illustrate the results.

1. Introduction

Frequency domain analysis of nonlinear systems appears to have developed from two main points of view, the quasi-linear describing function approach, and the more general but less amenable approach using the Volterra model. A third, (and in some ways intermediate) approach, has been to orthogonalise the Volterra kernels for some given input, the most well known example being the Wiener model for Gaussian inputs. Although each has certain benefits, there is no single, universally applicable, approach.

The describing function method, for example, has the considerable advantage of being one dimensional in frequency, [Atherton 1975], [Gelb, Vander Velde 1968]. Thus input and output components at the same frequency are related by a transfer function which, though amplitude dependent, is otherwise similar in form to the familiar linear case. Although this might suggest that input frequencies pass independently through the system, in reality any intermodulations or other frequency interactions have been incorporated, (or avoided), by restricting the input to a specific waveform. A describing function therefore is only stricly valid for a specified input, (such as a single sinusoid), and hence is limited in its generality. For the same reason the analysis becomes more complicated if the input considered contains more frequency components, and the method is rarely extended beyond the two tone case.

By contrast the n-dimensional Volterra transfer function explicitly describes nonlinear frequency interaction through the n frequency components which constitute its

arguments. The Volterra form therefore is not restricted to a particular input waveform, but this generality is achieved only by moving to higher dimensional representations [Volterra 1959]. In spite of recent interpretations [Peyton Jones, Billings], these multi-dimensional forms are not easy to assimilate, particularly for higher orders.

The advantages of the describing function approach could however be combined with those of the Volterra model, if, for any specified input, the multi-dimensional form could be collapsed down to the appropriate uni-dimensional response. Thus any number of specific describing functions could be derived from a more general model of the Volterra form.

Wiener and Spina (1980), for example, derive expressions for the Single Sinusoid Describing Function in terms of the Volterra kernels, and in this paper the approach is generalised for a wider class of inputs. In cases where the precise form of the input is not known, a similar method is used to derive a uni-dimensional response with bounds of uncertainty to accomodate the *range* of possible inputs. These methods therefore, in conjunction with recent algorithms for the computation of higher order transfer functions [Billings, Peyton Jones], provide a powerful means for deriving describing functions for a wide class of inputs.

2. The Volterra Model: Intra-, and Inter-Kernel Interference

Consider first the Volterra model representation for a single input analytic system, namely,

$$y(t) = \sum_{n=1}^{N} y_n(t) \tag{1}$$

where $y_n(t)$, the n-th order output of the system, is defined by,

$$y_n(t) = \int_{-\infty}^{\infty} \cdots \int_{-\infty}^{\infty} h_n(\tau_1, \cdots, \tau_n) \prod_{i=1}^{n} u(t-\tau_i)\, d\tau_i \tag{2}$$

Since the n-th order impulse response, $h_n(\cdot)$, is the Fourier pair of the n-th order transfer function, $H_n(\cdot)$, equation (2) may also be written as,

$$y_n(t) = \frac{1}{(2\pi)^n} \int_{-\infty}^{\infty} \cdots \int_{-\infty}^{\infty} Y_n(j\omega_1, \cdots, j\omega_n)\, e^{j(\omega_1 + \cdots + \omega_n)t}\, d\omega_1 \cdots d\omega_n \tag{3}$$

where,

$$Y_n(j\omega_1, \cdots, j\omega_n) = H_n(j\omega_1, \cdots, j\omega_n) \prod_{i=1}^{n} U(j\omega_i) \tag{4}$$

Notice that each harmonic/intermodulation (generated by interacting input frequency components) excites a unique point in the multi-dimensional frequency domain, corresponding to the cartesian product $\prod U(j\omega_i)$. The multidimensional spectrum $Y_n(j\omega_1, \cdots, j\omega_n)$ therefore contains a precise description of all input frequency interactions, but it is not immediately apparent how this relates to the the uni-dimensional output spectrum $Y_n(j\omega)$.

Consider however the change of variables given by,

$$\omega'_n = \sum_{i=1}^{n} \omega_i \qquad \Rightarrow \qquad \omega_n = \omega'_n - \sum_{i=1}^{n-1} \omega_i \tag{5}$$

Equation (3) may then be expressed in the 'input/output domain', $\omega_1, \cdots, \omega_{n-1}, \omega'_n$ as,

$$y_n(t) = \frac{1}{(2\pi)^n} \int_{-\infty}^{\infty} \cdots \int_{-\infty}^{\infty} Y_n(j\omega_1, \cdots, j\omega_{n-1}, j[\omega'_n - \sum_{i=1}^{n-1} \omega_i])\, e^{j\omega'_n t}\, d\omega_1, \cdots, d\omega_{n-1}, d\omega'_n \tag{6}$$

This shows more clearly how the uni-dimensional output spectrum is obtained, since equation (6) is in the form of an inverse Fourier transform. Hence the output spectrum is given by,

$$Y_n(j\omega'_n) = \frac{1}{(2\pi)^{n-1}} \int_{-\infty}^{\infty} \cdots \int_{-\infty}^{\infty} Y_n(j\omega_1, \cdots, j\omega_{n-1}, j[\omega'_n - \sum_{i=1}^{n-1} \omega_i])\, d\omega_1, \cdots, d\omega_{n-1} \tag{7}$$

and the variable ω'_n defines the observed output frequency.

In some cases it may be convenient to change variables entirely into the 'output domain' $\omega'_1, \cdots, \omega'_n$ according to,

$$\omega'_k = \sum_{i=1}^{k} \omega_i \qquad \Rightarrow \qquad \omega_i = \begin{cases} \omega'_i - \omega'_{i-1} & 1 < i \leq n \\ \omega'_i & i = 1 \end{cases} \tag{8}$$

This yields an alternative expression for the uni-dimensional output spectrum, namely,

$$Y_n(j\omega'_n) = \frac{1}{(2\pi)^{n-1}} \int_{-\infty}^{\infty} \cdots \int_{-\infty}^{\infty} Y_n(j\omega'_1, j[\omega'_2 - \omega'_1], \cdots, j[\omega'_n - \omega'_{n-1}])\, d\omega'_1 \cdots d\omega'_{n-1} \tag{9}$$

Geometrically both equations (7) and (9) represent the vector integration of points of response which lie within a sub-domain of constant output frequency, and which

therefore contribute to the same output frequency. The vectorial nature of this process defines an interference effect between output components of the same frequency which is termed intra-kernel interference, [Peyton Jones, Billings].

The total output response is however given by a summation of the n-th order responses, since by Fourier transform of equation (1),

$$Y(j\omega) = \sum_{n=1}^{N} Y_n(j\omega) \tag{10}$$

This combination of (one-dimensional) n-th order output responses does not involve any further intermodulation or transfer of energy between frequencies. However since the output components from different orders are vector quantities, the summation of equation (10) does introduce an amplitude dependent interference effect between the kernels termed 'inter-kernel interference', [Peyton Jones, Billings].

To illustrate this amplitude dependence consider an input waveform scaled by a constant factor A_w. Each n-th order output $Y_n(j\omega)$, being homogeneous, is therefore scaled by the constant factor A_w^n. Equation (10) then becomes,

$$Y(A_w, j\omega) = \sum_{n=1}^{N} A_w^n \, Y_n(j\omega) \tag{11}$$

Thus for example the summation of three kernel outputs at a given frequency ω_a could be depicted by the vector diagram, Figure 1(a). By doubling the input amplitude, the linear phasor $Y_1(j\omega)$ doubles, the second order output $Y_2(j\omega)$ quadruples, and so on. This results in an unequal scaling of the phasor contributions of each n-th order output, and considerably modifies both the magnitude and phase of the total output $\mathbf{Y}$, (as shown, half scale, in Figure 1(b)). These diagrams also illustrate how inter-kernel interference is sometimes sub-classified according to gain compression/expansion and phase advancement/retardation, through a comparison of the resultant output vector $\mathbf{Y}$ with the linear component $\mathbf{Y}_1$.

3. Generalised Describing Functions

The output response resulting from inter-kernel interference has close links with the describing function approach to nonlinear systems analysis. The latter is a quasi-linear (but amplitude dependent) transfer function relating input and output components at the same frequency,

$$N(A_w,j\omega) = \frac{Y(A_w,j\omega)}{A_w\, U(j\omega)} \tag{12}$$

Equation (12) might suggest that input frequencies pass independently through the system, whereas in reality there may be considerable interaction through intermodulations and intra-kernel interference. For this reason the describing function definition is restricted to a specific input waveform such as, for example, a single sinusoid. More generally however, equations (53),(12) may be combined to give,

$$N(A_w,j\omega) = \frac{1}{U(j\omega)} \sum_{n=1}^{N} A_w^{n-1}\, Y_n(j\omega) \tag{13}$$

where $N(A_w,j\omega)$ is considered to be undefined at any frequencies $U(j\omega) = 0$. Note that the spectrum $Y_n(j\omega)$ is given by the intra-kernel equation (34), and therefore accomodates any given frequency combination.

Expanding the first term of equation (13) yields,

$$N(A_w,j\omega) = H_1(j\omega) + \frac{1}{U(j\omega)} \sum_{n=2}^{N} A_w^{n-1}\, Y_n(j\omega) \tag{14}$$

Thus the describing function is given by the linear response, whose gain and phase are modified by the inter-kernel interference terms of higher order.

While equation (14) may be illustrated by the phasor diagrams similar to those of the previous section, the describing function representation enables input and output to be related more directly. For example the amplitude dependence of gain compression/expansion at a given frequency may be illustrated using a 'gain response curve' as shown in Figure 2(a). If the system were in fact linear, then the input/output amplitudes would be related by the dotted straight line of the figure, whose gradient is indeed the linear gain $|H_1(j\omega)|$. Nonlinear components modify this response, giving an augmented output (gain expansion) at points above the dotted line, or a decreased output (gain compression) below it. The two marked points correspond to the phasor plots Figures 1(a),(b), and demonstrate how these curves may be obtained by evaluating equation (53) at different input amplitudes.

The effect of amplitude on phase advancement/retardation may also be depicted in a similar manner by means of a 'phase response curve' as shown in Figure 2(b). In this case the linear phase is independent of input amplitude, giving the horizontal dotted line of the figure. However inter-kernel interference from nonlinear components in the

output can cause phase advancement, raising the curve above the dotted linear response, or retardation which lowers it. Again the marked points on the figure correspond to the phasor plots Figures 1(a),(b) which illustrate the interference mechanism at any given amplitude.

4. Multi-Sinusoidal Describing Functions with D.C. Bias. (MSDF)

Since the generalised describing function is constructed from the set of uni-dimensional spectra $Y_n(j\omega)$, the derivation of any specific describing function fundamentally involves derivation of the n-th order output spectrum generated by the specified input. Consider then a nonlinear system excited by an ordered set of sinusoids together with a d.c. offset,

$$u(t) = \sum_{r=1}^{R} A_r \cos(\omega_r t) + A_{d.c} \qquad \omega_i > \omega_j \quad \forall\, i > j \tag{15}$$

Although the harmonic expansion of the Volterra model could be obtained by applying the input (15) in the time domain, it is more convenient to derive the expansion in the frequency domain. Taking the Fourier transform of the input gives,

$$U(j\omega) = \sum_{r=1}^{R} A_r \pi[\delta(\omega-\omega_r) + \delta(\omega+\omega_r)] + 2\pi A_{d.c}\delta(\omega) = \sum_{r=-R}^{R} 2\pi \frac{A_{|r|}}{2} \delta(\omega-\omega_r) \tag{16}$$

where the latter equality follows by defining,

$$\omega_{-r} = -\omega_r \qquad \omega_0 = 0 \qquad \textit{and} \qquad A_0 = 2A_{d.c} \tag{17}$$

The product of input spectra is then a sum of delta functions,

$$\prod_{i=1}^{n} U(j\omega_i) = (2\pi)^n \sum_{r_1,r_n=-R}^{R} \prod_{i=1}^{n} \frac{A_{|r_i|}}{2} \delta(\omega_i-\omega_{r_i}) \tag{18}$$

which describe all those points in the multi-dimensional frequency domain which are excited into response. The n-dimensional output spectrum generated thereby is given from (3) as,

$$Y_n(j\omega_{r_1}, \cdots, j\omega_{r_n}) = (2\pi)^n \sum_{r_1,r_n=-R}^{R} \prod_{i=1}^{n} \frac{A_{|r_i|}}{2} \delta(\omega_i-\omega_{r_i})\ H_n(j\omega_1, \cdots, j\omega_n) \tag{19}$$

In this case the uni-dimensional output is most easily obtained by applying the integration (7), which by virtue of the delta functions in (19) is particularly simple to evaluate, and yields,

$$Y_n(j\omega'_n) = 2\pi \sum_{r_1,r_n=-R}^{R} \prod_{i=1}^{n} \frac{A_{|r_i|}}{2} H_n(j\omega_{r_1}, \cdots, j\omega_{r_{n-1}}, j[\omega'_n - \sum_{i=1}^{n-1}\omega_{r_i}]) \; \delta([\omega'_n - \sum_{i=1}^{n-1}\omega_{r_i}] - \omega_{r_n})$$

$$= 2\pi \sum_{r_1,r_n=-R}^{R} \prod_{i=1}^{n} \frac{A_{|r_i|}}{2} H_n(j\omega_{r_1}, \cdots, j\omega_{r_n}) \; \delta([\omega'_n - \sum_{i=1}^{n}\omega_{r_i}]) \qquad (20)$$

Thus the output spectrum consists of a series of spectral lines at those frequencies ω'_n, which satisfy the condition $\omega'_n = \sum\omega_{r_i}$. Indeed this confirms previous discussions [Peyton Jones, Billings].

Equation (20) however may be simplified by expressing the result in terms of the symmetric transfer function $H_n(\cdot)$. Dividing the multiple summation into two parts gives,

$$Y_n(j\omega'_n) = 2\pi \sum_{\substack{\text{all combinations} \\ \text{of freqs } \{\omega_{-R} \cdots \omega_R\} \\ \text{taken } n \text{ at a time}}} \; \sum_{\text{all permutations of } \{\omega_{r_1} \cdots \omega_{r_n}\}} \prod_{i=1}^{n} \frac{A_{|r_i|}}{2} H_n(j\omega_{r_1}, \cdots, j\omega_{r_n}) \; \delta([\omega'_n - \sum_{i=1}^{n}\omega_{r_i}]) \qquad (21)$$

Notice that the latter sum of permutations has no effect on the output frequency $\omega'_n = \sum\omega_{r_i}$, and merely combines the response of a set of asymmetric points. This summation can therefore be written in terms of the symmetric transfer function as,

$$\sum_{\substack{\text{all permutations} \\ \text{of } \{\omega_{r_1} \cdots \omega_{r_n}\}}} H_n(j\omega_{r_1}, \cdots, j\omega_{r_n}) = n^* \, H_n^{sym}(j\omega_{r_1}, \cdots, j\omega_{r_n}) \qquad (22)$$

where,

$$\begin{aligned} n^* &= \frac{n!}{n_1!\, n_2! \cdots n_c!} \\ c &= \textit{the number of distinct frequencies appearing in the combination} \\ n_i &= \textit{the number of repetitions of the ith distinct frequency} \\ n_1 + n_2 + \cdots + n_c &= n \end{aligned} \qquad (23)$$

Meanwhile the former sum of combinations may be generated from the initial multiple summation, but with all permutations excluded by the constraint $r_i \le r_{i-1}$. Equation (23) then becomes,

$$Y_n(j\omega'_n) = 2\pi \, n^* \sum_{\substack{r_1,r_n=-R \\ r_i \le r_{i-1}}}^{R} \prod_{i=1}^{n} \frac{A_{|r_i|}}{2} H_n^{sym}(j\omega_{r_1}, \cdots, j\omega_{r_n}) \; \delta([\omega'_n - \sum_{i=1}^{n}\omega_{r_i}]) \qquad (24)$$

The multi-sinusoidal describing function, defined at any of the input frequencies ω_r, can now be found by combining equations (14), (24) giving,

$$N(A_w,j\omega'_n) = H_1(j\omega'_n) + \frac{1}{A_r\pi\delta(\omega'_n-\omega_r)} \sum_{n=2}^{N} A_w^{n-1}.2\pi\, n^* \times \sum_{\substack{r_1,r_n=-R \\ r_i \le r_{i-1}}}^{R} \prod_{i=1}^{n} \frac{A_{|r_i|}}{2} H_n^{sym}(j\omega_{r_1}, \cdots, j\omega_{r_n})\, \delta([\omega'_n-\sum_{i=1}^{n}\omega_{r_i}]) \quad (25)$$

$$\Rightarrow N(A_w,j\omega_r) = H_1(j\omega_r) + \sum_{n=2}^{N} \frac{2A_w^{n-1}\, n^*}{A_r} \sum_{\substack{r_1,r_n=-R \\ r_i \le r_{i-1}}}^{R} \prod_{i=1}^{n} \frac{A_{|r_i|}}{2} H_n^{sym}(j\omega_{r_1}, \cdots, j\omega_{r_n})\, \delta([\omega_r-\sum_{i=1}^{n}\omega_{r_i}])$$

4.1. Harmonic input describing function (HIDF)

A particularly important sub-class of the input (15) is one in which the excitation frequencies are harmonically related, i.e,

$$\omega_r = r\omega_f \quad (26)$$

where ω_f denotes some fundamental frequency. Such inputs might arise through feedback round some nonlinear system (as in limit cycle analysis), or by cascading the output of one nonlinear system to the input of another. More importantly though, equations (26),(15) serve to characterise a wide range of periodic signals by means of their Fourier Series representation. A harmonic input describing function could then be applied to yield the describing function for specific periodic waveforms, e.g triangular, square etc.

The time domain derivation of the HIDF is complicated by the large number of intermodulations generated by such inputs. However substituting (10) in (25) gives in the frequency domain, (27)

$$N(A_w,jr\omega_f) = H_1(jr\omega_f) + \sum_{n=2}^{N} \frac{2A_w^{n-1}\, n^*}{A_r} \sum_{\substack{r_1,r_n=-R \\ r_i \le r_{i-1}}}^{R} \prod_{i=1}^{n} \frac{A_{|r_i|}}{2} H_n^{sym}(jr_1\omega_f, \cdots, jr_n\omega_f)\, \delta([r-\sum_{i=1}^{n}r_i])$$

This expression may be simplified by reflecting the constraint, $r=\sum r_i$ (imposed by the delta function), back to the choice of arguments r_i (generated by the multiple summation). The required condition may be rewritten,

$$r_i = r - \sum_{k=1}^{i-1} r_k - \sum_{k=i+1}^{n} r_k \quad (28)$$

where by use of recursion, only the latter summation is unknown. However since all input frequencies lie in the range $\pm\omega_R$, the maximum value of the unknown summation, having $(n-i)$ elements, is $(n-i)R$. Similarly the condition $r_i \le r_{i-1}$ gives a minimum value for summation of $(n-i)r_{i-1}$. Hence (28) becomes,

$$r - \sum_{k=1}^{i-1} r_k - (n-i)R \;\le\; r_i \;\le\; r - \sum_{k=1}^{i-1} r_k + (n-i)R \tag{29}$$

Combining (29) and (27) therefore enables the HIDF to be expressed in the form,

$$N(A_w, jr\omega_f) \;=\; H_1(jr\omega_f) + \sum_{n=2}^{N} 2A_w^{n-1} n^* \sum_{r_1, r_n = r_{\min}}^{r_{\max}} \prod_{i=1}^{n} \frac{A_{|r_i|}}{2}\, H_n^{sym}(jr_1\omega_f, \cdots, jr_n\omega_f) \tag{30}$$

where,

$$r_{\min} \;=\; max \begin{cases} -R, \\ r - \sum_{k=1}^{i-1} r_k - (n-i)r_{i-1} \end{cases} \qquad r_{\max} \;=\; min \begin{cases} R, \\ r_{i-1}, \\ r - \sum_{k=1}^{i-1} r_k + (n-i)R \end{cases} \tag{31}$$

Although restricted to harmonic inputs, equations (26),(15) define an important class of describing functions, and a number of common instances are discussed below.

4.1.1. *Single sinusoidal describing function (SSDF)*

The simplest sub-class of the input (26) occurs when the system is excited by a single sinusoid alone, i.e. R=1, and $r_i \neq 0$ (no d.c. input). Applying these values in equations (30),(31) yields the SSDF for the fundamental frequency ω_1, giving,

$$\begin{aligned} N(A_w, j\omega_1) \;=\; H_1(j\omega_1) \;+\; & \frac{3}{4} A_w^2 H_3^{sym}(j\omega_1, j\omega_1, -j\omega_1) \\ & + \frac{5}{8} A_w^4 H_5^{sym}(j\omega_1, j\omega_1, j\omega_1, -j\omega_1, -j\omega_1) \;+\; \cdots \end{aligned} \tag{32}$$

where, for clarity, the amplitude A_1 has been absorbed into the waveform scaling factor A_w. This result is not new ([Weiner, Spina 1980]). The advantage of (30),(31) however is the ease with which it can be be applied to generate describing functions for more complicated inputs.

4.1.2. *Biassed single sinusoidal describing function (BSSDF)*

Consider for example a Biassed Single Sinusoid Describing Function (BSSDF), where the input consists of a sinusoid together with a d.c bias offset. Such inputs are of interest in simple limit cycle analysis where the nonlinearity is excited by a sinusoidal component from the limit cycle, together with a relatively slow varying command input (approximated by the d.c. bias).

Expanding (30),(31) with R=1, (single sinusoid), and including a d.c. component by permitting r_i=0, gives the Volterra expansion for the BSSDF:

$$N(A_w,A_1,A_{d.c},j\omega_1) = H_1(j\omega_1) + 2\,A_wA_{d.c}\,H_2^{sym}(j\omega_1,0) + \left[\,\frac{3}{4}\,A_w^2A_1^2\,H_3^{sym}(j\omega_1,j\omega_1,-j\omega_1) + 3\,A_w^2A_{d.c}^2\,H_3^{sym}(j\omega_1,0,0)\,\right] + \cdots \tag{33}$$

Notice that with more than one frequency component in the input, the individual amplitudes A_r cannot be absorbed within the waveform scaling factor A_w, and each appears explicitly in equation (33). This is because changing the amplitude of any input component alters the input waveform *shape*, while changing the factor A_w preserves the amplitude ratio between input components and merely *scales* the input waveform without distortion.

4.1.3. *Twin sinusoidal describing function (TSDF)*

The BSSDF is really a special case of the twin or two-tone sinusoidal describing function (TSDF), only in the latter case both input components may occur at any frequency. Consider for example a nonlinear system excited by two harmonically related sinusoids such that $\omega_3 = 3\omega_1$ (or $\omega_1 = \omega_3/3$). A separate describing function may be defined for each of these input frequencies. Thus expanding (30),(31) for the lower of the two frequencies, ω_1, gives the fundamental describing function,

$$N(A_w,A_1,A_3,j\omega_1) = H_1(j\omega_1) + \frac{6}{4}\,A_w^2A_3^2\,H_3^{sym}(j\omega_3,j\omega_1,-j\omega_3) + \frac{3}{4}\,A_w^2A_1A_3\,H_3^{sym}(j\omega_3,-j\omega_1,-j\omega_1) + \frac{3}{4}\,A_w^2A_1^2\,H_3^{sym}(j\omega_1,j\omega_1,-j\omega_1) + \cdots \tag{34}$$

where the condition $r_i \neq 0,\pm 2$ excludes d.c. and first harmonic components from the input.

Similarly expanding (30),(31) with r=3 yields the describing function at the higher

frequency ω_3:

$$N(A_w,A_1,A_3,j\omega_3) = H_1(j\omega_3) + \frac{6}{4}\frac{A_w^2A_3^2}{A_1} H_3^{sym}(j\omega_3,j\omega_3,-j\omega_3) + \tag{35}$$

$$\frac{3}{4} A_w^2A_1A_3\, H_3^{sym}(j\omega_3,j\omega_1,-j\omega_1) + \frac{3}{4} A_w^2A_1^2\, H_3^{sym}(j\omega_1,j\omega_1,j\omega_1) + \cdots$$

Such illustrative examples, though fairly straightforward, may be extended to higher orders and to inputs with greater frequency content.

4.1.4. *Fourier series describing function: triangular wave example*

A particularly useful feature of HIDF analysis is the ability to derive the describing function for a periodic input represented by a Fourier series, following a similar approach to the simple two-tone case above. Consider for example a triangular wave input which may be represented by its Fourier series as,

$$u(t) = \frac{8A_T}{\pi}\left(\cos\omega_f t + \frac{1}{9}\cos 3\omega_f t + \frac{1}{25}\cos 5\omega_f t + \cdots\right) \tag{36}$$

The HIDF for such a series is obtained from (30),(31) , with the restriction r_i is always odd and A_w=1, giving,

$$N(A_1,A_2,A_5,j\omega_f) = H_1(j\omega_f) \tag{37}$$

$$\frac{6}{4} A_5^2\, H_3^{sym}(5j\omega_f,j\omega_f,-5j\omega_f) + \frac{3}{4}\frac{A_5A_3^2}{A_1} H_3^{sym}(3j\omega_f,3j\omega_f,-5j\omega_f) +$$
$$+ \frac{6}{4} A_5A_3\, H_3^{sym}(5j\omega_f,-j\omega_f,-3j\omega_f) + \frac{6}{4} A_3^2\, H_3^{sym}(3j\omega_f,j\omega_f,-3j\omega_f) +$$
$$\frac{3}{4} A_1A_3\, H_3^{sym}(3j\omega_f,-j\omega_f,-j\omega_f) + \frac{3}{4} A_1^2\, H_3^{sym}(j\omega_f,j\omega_f,-j\omega_f) + \cdots$$

In this case however, the amplitudes $A_0, \cdots, A_n$ of the HIDF are all related the the amplitude A_T of the triangular wave by the Fourier coefficients of (36). Equation (37) may therefore be simplified to give the Triangular Describing Function, (TDF),

$$N(A_T,j\omega_f) = H_1(j\omega_f)$$
$$+ \left[\frac{8A_T}{\pi}\right]^2 \left[\begin{array}{l} \frac{3}{1250} H_3^{sym}(5j\omega_f,j\omega_f,-5j\omega_f) + \frac{1}{900} H_3^{sym}(3j\omega_f,3j\omega_f,-5j\omega_f) + \\ \frac{1}{150} H_3^{sym}(5j\omega_f,-j\omega_f,-3j\omega_f) + \frac{1}{54} H_3^{sym}(3j\omega_f,j\omega_f,-3j\omega_f) + \\ \frac{1}{12} H_3^{sym}(3j\omega_f,-j\omega_f,-j\omega_f) + \frac{3}{4} H_3^{sym}(j\omega_f,j\omega_f,-j\omega_f) \end{array}\right]$$

$$+ \cdots \tag{38}$$

Note that specific expansions such as (33),(34),(35),(38) are merely illustrative of the method for generating various describing functions from the Volterra form. In practice the recursive algorithm is well suited for computer implementation, and avoids these tediously longwinded expressions.

4.1.5. *Examples*

Consider for example the continuous time nonlinear resonator given by,

$$\frac{d^2y}{dt^2} + 2\zeta\omega_n\frac{dy}{dt} + \omega_n^2 y - \omega_n^2 u + 0.02\omega_n^2 u^2 + 0.01\omega_n^2 u^2\frac{du}{dt} = 0 \tag{39}$$

where $\omega_n = \pm 100\pi/3$, $\zeta = 0.2$. The nonlinearity is deliberately severe so that the differences between the various describing functions are readily apparent, even when evaluated with modest input amplitudes and plotted on logarithmic scales. In particular the differential factor in the cubic term might be expected to accentuate high frequency input components, and indeed this is confirmed by the results obtained below.

The first stage of analysis concerns the derivation of the generalised frequency response functions. The first order transfer function is obtained from (39) by ignoring all the nonlinear terms, giving,

$$H_1(j\omega) = \frac{\omega_n^2}{(j\omega)^2 + 2\zeta\omega_n(j\omega) + \omega_n^2} \tag{40}$$

Higher orders however may be found using the algorithms developed in [Billings, Peyton Jones], though the results in this case are quite straightforward. For example the second order response shares the same characteristic equation as the linear response, but with ω in the latter replaced by $\omega_1+\omega_2$, giving,

$$H_2^{sym}(j\omega_1,j\omega_2) = \frac{0.02\omega_n^2}{(j\omega_1+j\omega_2)^2 + 2\zeta\omega_n(j\omega_1+j\omega_2) + \omega_n^2} \tag{41}$$

Similar properties apply to the third order transfer function, generated by the cubic

term of equation (41). However the differential factor also introduces a zero into the numerator of the transfer function, giving,

$$H_3^{sym}(j\omega_1,j\omega_2,j\omega_3) = \frac{0.01\omega_n^2}{3} \times \frac{(j\omega_1 + j\omega_2 + j\omega_3)}{(j\omega_1+j\omega_2+j\omega_3)^2 + 2\zeta\omega_n(j\omega_1+j\omega_2+j\omega_3) + \omega_n^2} \qquad (42)$$

Finally since the system under consideration contains no 'recursive' nonlinearities in the output $y(t)$, the response of all orders fourth and higher, is zero.

These generalised transfer functions explicity describe frequency and amplitude non-linearities without restriction to a specific input waveform, but only at the expense of multi-dimensional forms. However such generality may be exploited to derive any number of specific (uni-dimensional) describing functions from this single Volterra representation.

For example, combining equations (40)-(42) with (32) yields the single sinusoidal describing function for the system (39), as plotted (solid line) in Figure (3). Notice by comparison with the linear response, (dotted line), that the system exhibits increasing gain expansion with frequency, coupled with significant phase retardation.

Introducing now a d.c. bias component gives from (33) the BSSDF, which is shown in Figure (4). The trends observed in the single sinusoid case are accentuated by the presence of the d.c. component, and could for example reduce the gain and phase margins in a control application, or even cause instability.

In other applications, where the input consists of two harmonically related sinusoids, the appropriate describing function can still be obtained from the general form (40)-(42). Thus the TSDF described in Section 4.1.3 can be evaluated for the system (39), and gives the fundamental describing function shown in Figure (5). The TSDF can also be evaluated for the higher harmonic using equation (35), and this is shown in Figure (6). Notice that the describing function associated with the higher component exhibits more nonlinearity than that of the fundamental, confirming the trend of high frequency distortion.

Finally the describing function for any given periodic waveform can be obtained for the system (39) by representing the input as a Fourier series. The triangular describing function of equation (38) is obtained in this way, and gives for this system the response shown in Figure (7). Notice from (36) that the triangular waveform

excitation is concentrated at the fundamental, and consequently the TDF of Figure 7 is very similar to that obtained for the single sinusoid case.

5. White Noise Describing Functions

The multi-sinusoidal describing function of Section 4 demonstrated how the generalised describing function approach may be applied to the specific class of inputs (26),(15). Another form of input worthy of consideration consists of white noise excitation with variance A and bandwidth ω_b. This input has a flat spectrum of amplitude A, and excites every point of the transfer function into the response. Indeed using equation (5) the output spectrum (39) may be rewritten, (43)

$$Y_n(\omega) = \frac{A^n}{(2\pi)^{n-1}} \int_{max\ \{-i\omega_b,(\omega_{i+1}-\omega_b)\}}^{min\ \{i\omega_b,(\omega_{i+1}+\omega_b)\}} \cdots \int H_n(j\omega'_1, j[\omega'_2-\omega'_1], \cdots, j[\omega'_n-\omega'_{n-1}])\, d\omega'_1 \cdots d\omega'_{n-1}$$

Notice how the input domain bounds $\pm\omega_b$ are transformed in the output domain integration of equation (43). These new limits were obtained by applying the input constraint on equation (8), giving

$$|\omega'_i| \le i\omega_b \qquad 1 \le i \le n \tag{44}$$

$$\omega_b \ge \begin{cases} |\omega'_i - \omega'_{i-1}| & 1 < i \le n \\ |\omega'_i| & i = 1 \end{cases} \tag{45}$$

Since the output frequency ω'_n is fixed, equation (45) may be rewritten with shifted indices and rearranged to give,

$$|\omega'_i| \ge |\omega'_{i+1}| - \omega_b \qquad 1 \le i \le n-1 \tag{46}$$

which then defines the new integral limits of equation (43).

Combining equations (14), (43) therefore gives the white noise describing function,

$$N(A,j\omega) = H_1(j\omega) + \sum_{n=2}^{N} A^{n-1} \int_{max\ \{-i\omega_b,(\omega_{i+1}-\omega_b)\}}^{min\ \{i\omega_b,(\omega_{i+1}+\omega_b)\}} \cdots \int H_n(j\omega'_1, j[\omega'_2-\omega'_1], \cdots, j[\omega-\omega'_{n-1}])\, d\omega'_1 \cdots d\omega'_{n-1} \tag{47}$$

It is perhaps surprising, in view of the comprehensive excitation provided by a white noise input, that (47) does not necessarily give the worst case describing function of any input within the spectral amplitude A, and bandwith ω_b. This is because the

complex/vector integration of all points within the given sub-domain of constant output frequency ω, causes intra-kernel interference between all these components. Depending on the exact form of $H_n(\cdot)$ they may act constructively, but equally it is possible that they may act destructively, with one intermodulation cancelling the effect of another. The white noise response therefore does not necessarily give the worst case output, and cannot guarantee that every nonlinear mode reaches the final output. However the concept of a worst case describing function could be useful, and is further developed below.

6. Worst Case Describing Functions

Although the describing function forms introduced above encompass a wide class of inputs, any specific application requires a particular and well defined input. In many cases however the precise form of the input is not known. Indeed it is for this reason that the Volterra transfer functions are multi-dimensional in frequency so that any possible input combination may be accomodated. An alternative approach however might be to sacrifice the detail of such descriptions for the clarity of the unidimensional response, and introduce instead bounds of uncertainty to accomodate a *range* of possible inputs. Of course if an interesting feature were detected in this 'worst case n-th order output', then the analyst could examine it in more detail by reverting to the multidimensional form.

A suitable class of inputs to consider might be defined as falling within a frequency bandwidth ω_b and spectral amplitude range $\leq A$. The worst case output can then be obtained in a manner similar to that already described for white noise, only in this case every point is forced to act constructively by integrating only the modulus of the frequency response, and assuming that all points are in phase,

(48)

$$Y_n^{worst}(\omega) = \frac{A^n}{(2\pi)^{n-1}} \int_{max\ \{-i\omega_b,(\omega_{i+1}-\omega_b)\}}^{min\ \{i\omega_b,(\omega_{i+1}+\omega_b)\}} \cdots \int |H_n(j\omega'_1, j[\omega'_2-\omega'_1], \cdots, j[\omega'_n-\omega'_{n-1}])|\, d\omega'_1 \cdots d\omega'_{n-1}$$

Thus the worst case input is similar to white noise in the sense that it excites every point of the n-th order transfer function into the response, but it has the additional property that its phase brings all these contributions in line so that they all act constructively. The resulting output spectrum then has a magnitude bound given by equation (48) and arbitrary phase.

Combining equations (14), (48) therefore gives the worst case describing function,

$$N(A,j\omega)^{worst} = H_1(j\omega) \tag{49}$$
$$+ \sum_{n=2}^{N} A^{n-1} \int_{max\ \{-i\omega_b,(\omega_{i+1}-\omega_b)\}}^{min\ \{i\omega_b,(\omega_{i+1}+\omega_b)\}} \cdots \int |H_n(j\omega'_1,j[\omega'_2-\omega'_1],\ \cdots\ ,j[\omega-\omega'_{n-1}])|\ d\omega'_1 \cdots d\omega'_{n-1}$$

Notice in this case that the linear response $H_1(\cdot)$ is modified by the magnitude bounds $Y_n^{worst}(\cdot)$, which have arbitrary phase. This lack of phase information also makes it impossible to distinguish between gain compression or expansion, or between phase advancement or retardation. Instead the worst case describing function gives circles of uncertainty of radius $\Delta H(\omega)$,

$$\Delta H(\omega) = \sum_{n=2}^{N} \Delta H_n(\omega) = \sum_{n=2}^{N} A^{n-1}\ Y_n^{worst}(\omega) \tag{50}$$

which are imposed on the linear response as shown in the phasor plot Figure 8. Notice that the maximum phase uncertainty $\Delta\phi(\omega)$, introduced by the nonlinearities, depends on the magnitude of the linear response, since by simple trigonometry from the figure,

$$\Delta\phi(\omega) \simeq arctan\left[\frac{\Delta H(\omega)}{|H_1(j\omega)|}\right] \tag{51}$$

Thus the bounds of the worst case describing function are most easily expressed as,

$$|N(A,j\omega)^{worst}| = |H_1(j\omega)| \pm \Delta H(\omega) \tag{52}$$

$$\angle N(A,j\omega)^{worst} = \angle H_1(j\omega) \pm \Delta\phi(\omega) \tag{52}$$

Notice that the gain and phase uncertainties, $\Delta H(\omega)$,$\Delta\phi(\omega)$, have the same amplitude dependence as any describing function, i.e. doubling the input amplitude, for example, doubles the second order uncertainty, quadruples that of the third order, and so on. This effect may be depicted using gain or phase response curves similar to those of Section 3, only in this case the curves themselves are replaced by bands of uncertainty as shown in Figure 9. However the existance of a well defined input at all frequencies within the specified bandwidth ensures that equation (49) is also well defined at all frequencies of interest. Thus the gain and phase response plots, which relate amplitude dependence at a constant input frequency, may be complemented by worst case Bode or Nyquist plots across all the frequencies of the bandwidth, but at constant amplitude.

6.1. Examples

Consider for example the continuous time nonlinear resonator given by,

$$\frac{d^2y}{dt^2} + 2\zeta\omega_n\frac{dy}{dt} + \omega_n^2 y - \omega_n^2 u + 0.01\omega_n^2 u^2 = 0 \qquad (53)$$

where as before $\omega_n = \pm 100\pi/3$, $\zeta = 0.2$. The system is similar to that discussed in Section 4.1.5, only in this case the nonlinearity is less severe in view of the greater degree of excitation, - namely any input within the bandwith $\omega_b = 100\pi$, and specral amplitude range $A \leq 0.8$.

Consequently the first order transfer function of (53) is identical to that given in equation (40), and the second order response is simply half that obtained previously giving,

$$H_2^{sym}(j\omega_1, j\omega_2) = \frac{0.01\omega_n^2}{(j\omega_1+j\omega_2)^2 + 2\zeta\omega_n(j\omega_1+j\omega_2) + \omega_n^2} \qquad (54)$$

The worst case second order output spectrum may now be found by integrating $|H_2(\cdot)|$ along sub-domains of constant output frequency according to equation (48), from which the gain uncertainty (50) is obtained. Combining this result with the linear response (40) also yields the phase uncertainty $\Delta\phi(\omega)$, (51). These results are plotted in the form of equation (52), with the linear response (dotted) surrounded by bands of uncertainty $\Delta H(\omega), \Delta\phi$ shown as solid lines (see Figure 10).

The bands are quite wide and may in practice be overly pessimistic. Nevertheless they do provide a useful overview of the system behaviour. For example the major uncertainty in this case is at low frequencies, and the dominant resonance still occurs at the linear resonant frequency.

Notice also that if more information were available concerning the system inputs, it might be possible to contract the bands of uncertainty by restricting the class of inputs considered. In the limit, where the input is known precisely, the bounds of uncertainty should converge on the deterministic describing function for that given input.

7. Conclusions

A brief overview of the analysis and interpretation of n-dimensional Volterra transfer functions has been given. Based on this understanding, relationships between the Volterra form and the uni-dimensional describing function representation have been

derived. These include specific algorithms for obtaining the general harmonic input describing function, and examples of its application to commonly used inputs (e.g. single sinusoid, sine + bias, two-tone and Fourier series) have been given. The same approach has been used to obtain an expression for the white noise describing function. Finally the describing function concept has been extended by means of a bounded worst-case transfer function.

When used in conjunction with recent algorithms for evaluating the Volterra transfer functions of nonlinear difference and differential equations, these expressions offer a useful means to obtain any number of specific describing functions from a single model form. The results obtained thereby may prove useful in more accurate limit cycle and stability analysis. In particular the worst-case describing function, though pessimistic, may prove useful in stability analysis and control system design.

References

ATHERTON, D.P., (1975). *Nonlinear Control Engineering*, Van Nostrand Reinhold, London.

BILLINGS, S.A. AND PEYTON JONES, J.C, "Mapping Nonlinear Integro-Differential Equations Into the Frequency Domain," *Int J. Control (to appear).*

GELB, A. AND VANDER VELDE, W.E., (1968). *Multiple-Input Describing Functions and Nonlinear System Design*, McGraw-Hill, New York.

PEYTON JONES, J.C. AND BILLINGS, S.A., "The Interpretation of Nonlinear Frequency Response Functions," *Int J. Control (to appear).*

VOLTERRA, V., (1959). *Theory of functionals and of integral and integrodifferential equations*, Dover, New York.

WIENER, D.D. AND SPINA, J.F., (1980). *Sinusoidal analysis and modelling of weakly nonlinear circuits*, Van Nostrand, New York.

$Y_1(j\omega_a) = 12.9\ 10^{-3} \angle 75°$
$Y_2(j\omega_a) = 6.7\ 10^{-3} \angle 30°$
$Y_3(j\omega_a) = 3.7\ 10^{-3} \angle -116°$

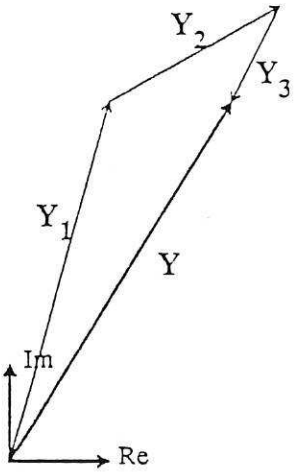

Fig 1(a)

$Y_1(j\omega_a) = 25.8\ 10^{-3} \angle 75°$
$Y_2(j\omega_a) = 26.8\ 10^{-3} \angle 30°$
$Y_3(j\omega_a) = 29.6\ 10^{-3} \angle -116°$

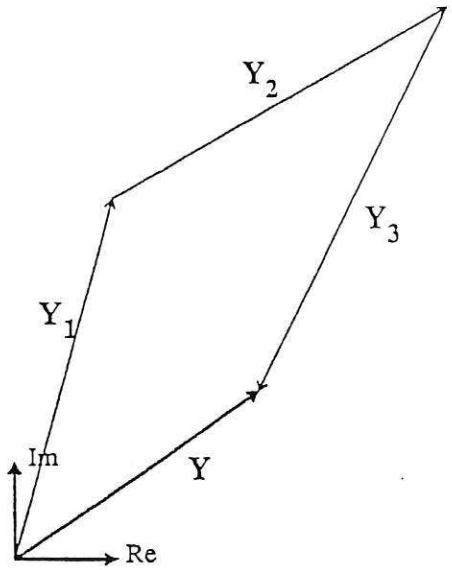

Fig 1(b) ($\frac{1}{2}$ scale).

Amplitude dependence of inter - kernal interference

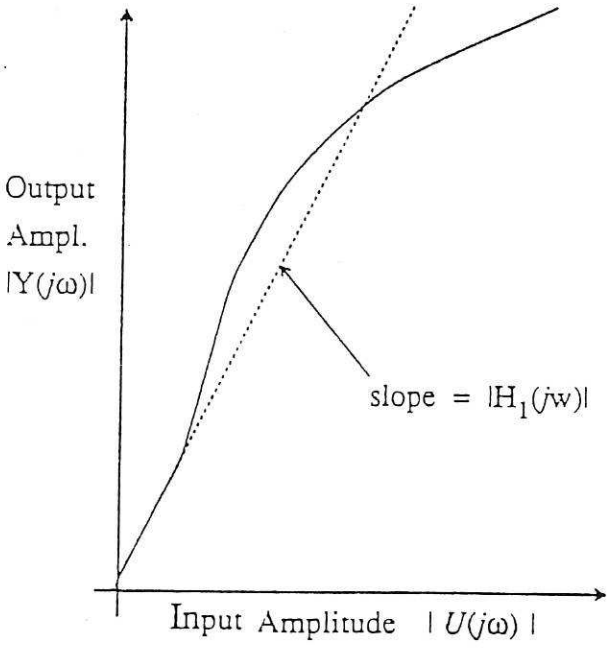

Fig 2(a) Gain response curve.

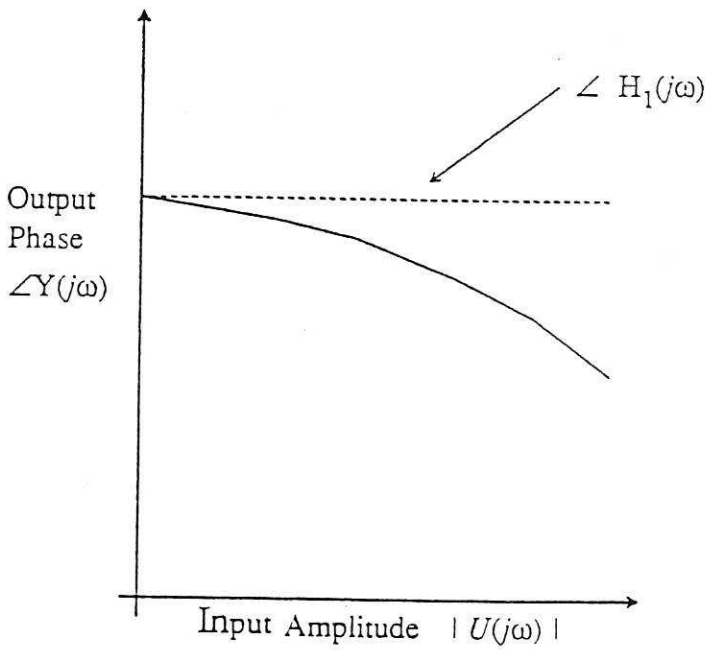

Fig 2(b) Phase response curve.

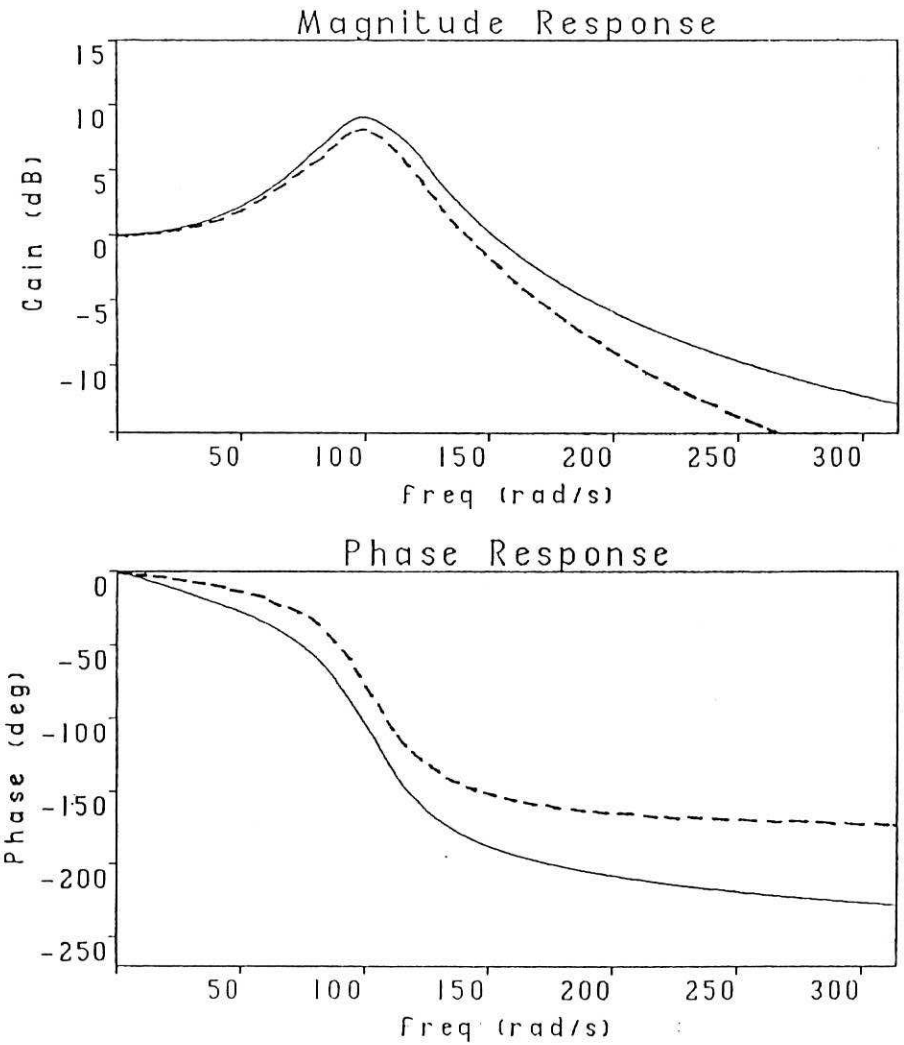

Fig 3 SSDF (A = 1.4)

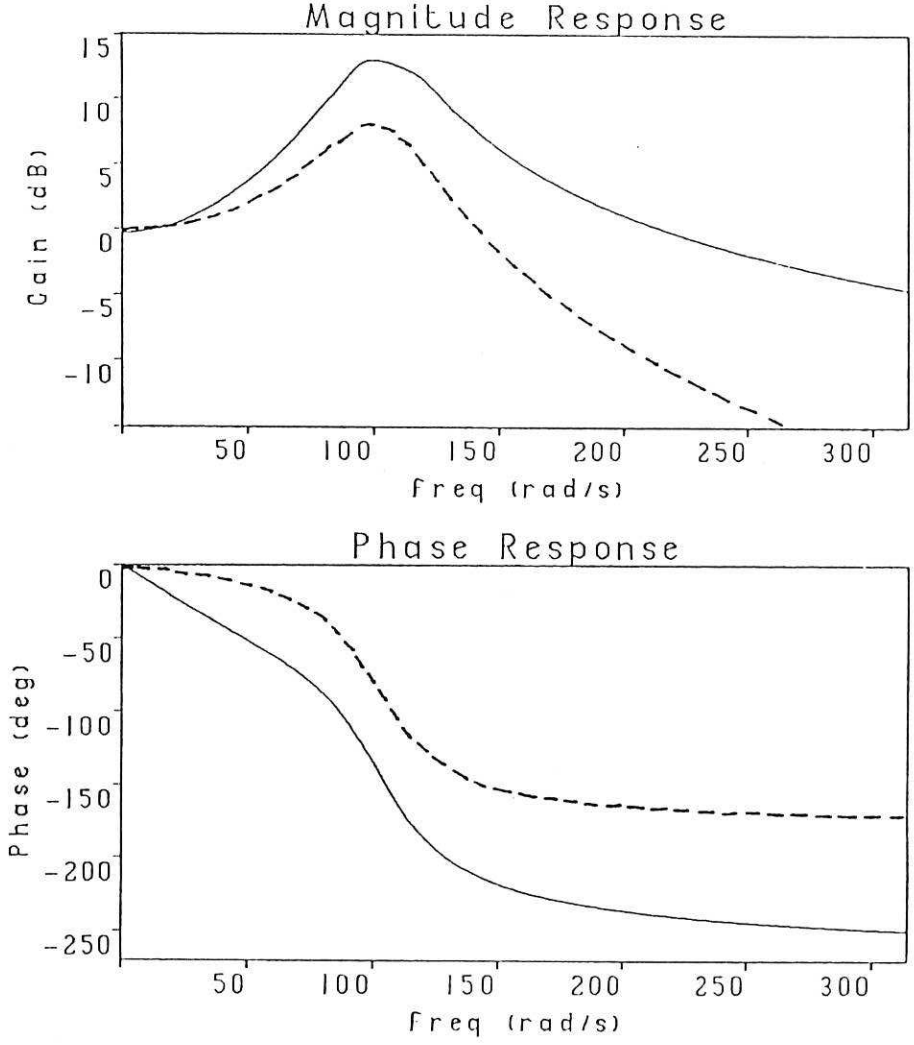

Fig 4 BSSDF ($A_0 = 1.0$, $A_1 = 1.4$).

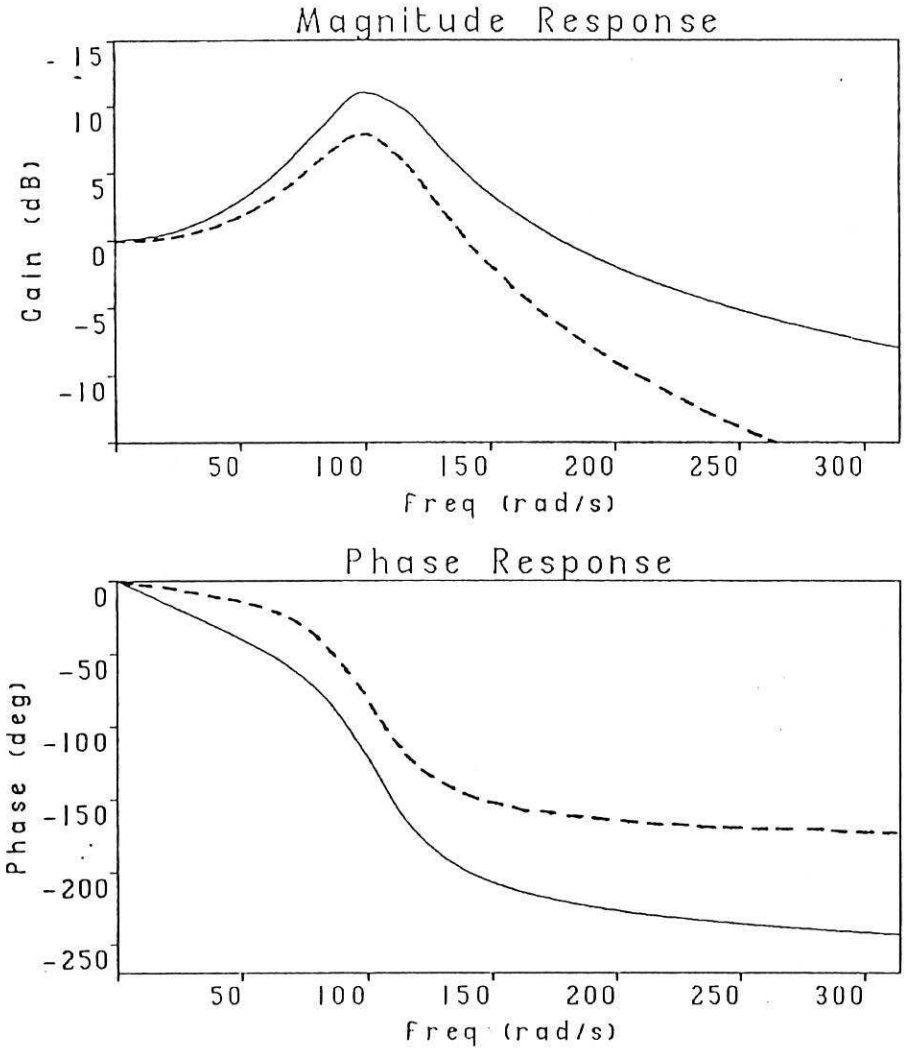

Fig 5 $TSDF_1$ ($A_1 = 1.4$, $A_3 = 0.7$).

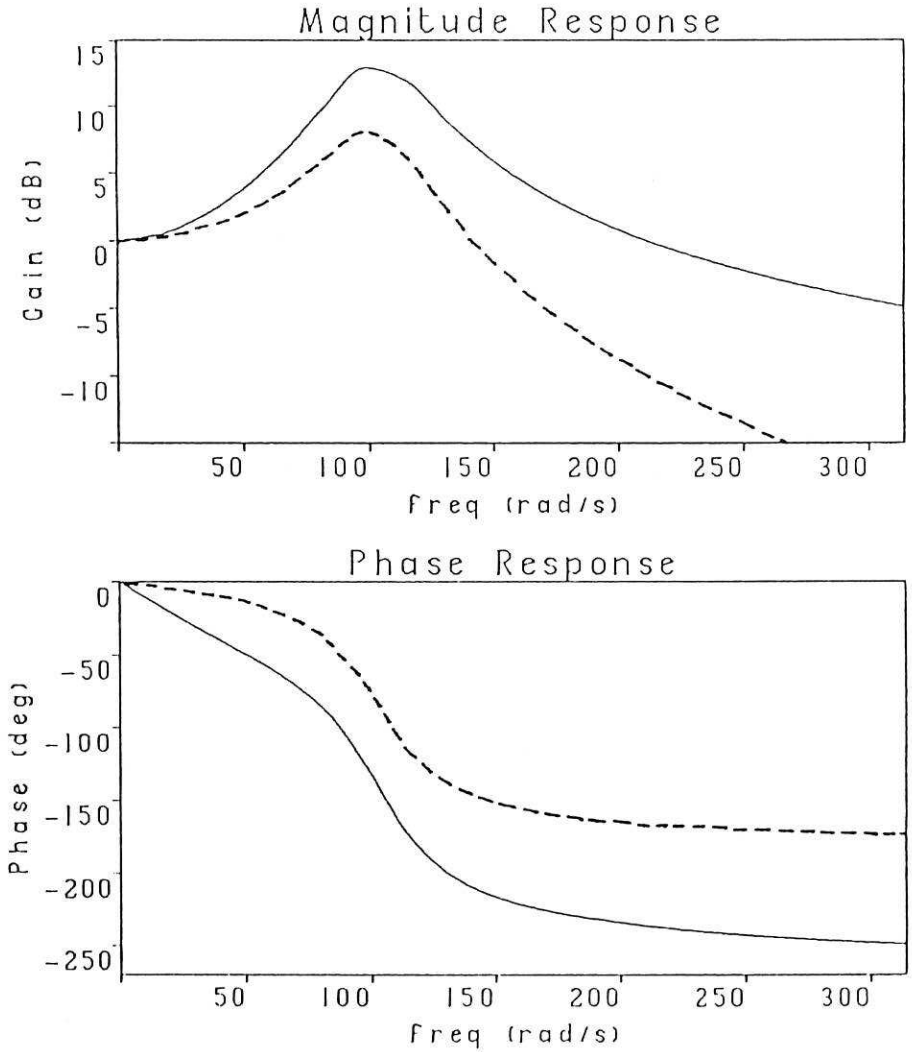

Fig 6 $TSDF_3$ ($A_1 = 1.4$, $A_3 = 0.7$).

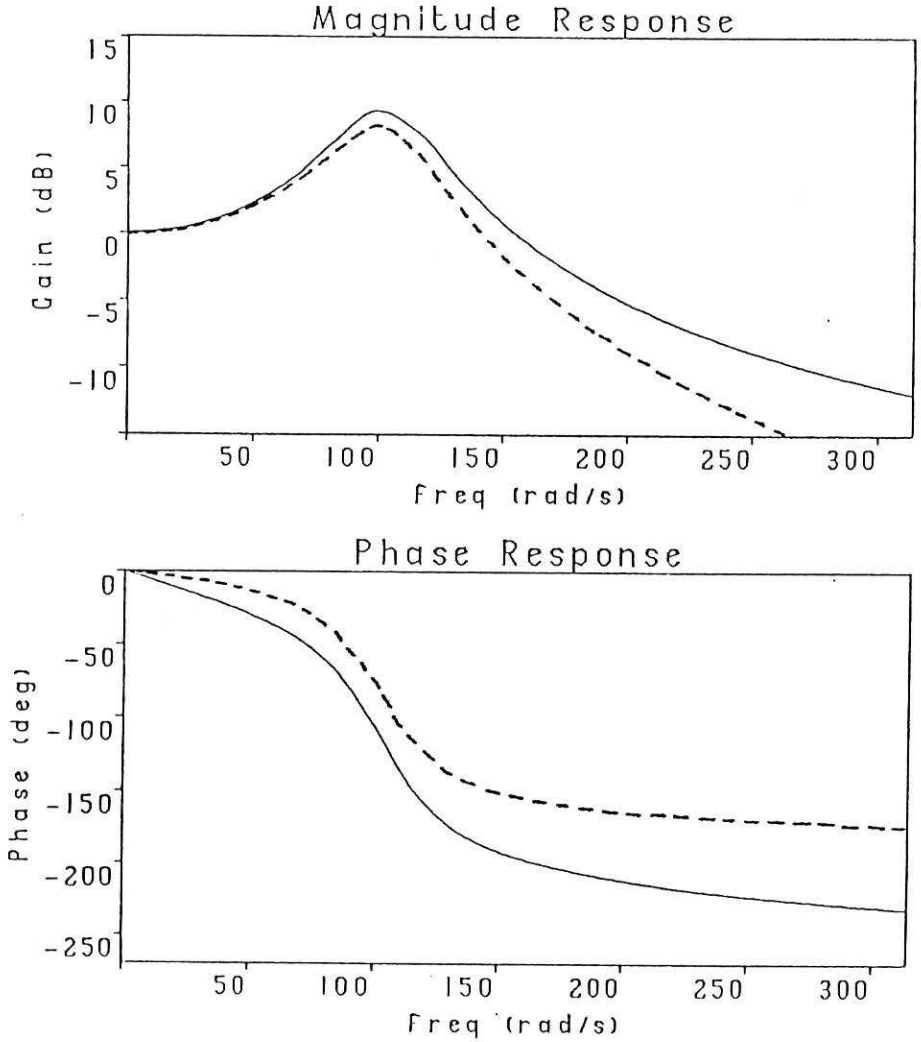

Fig 7 TDF ($A_T = \frac{1.4\pi}{8}$)

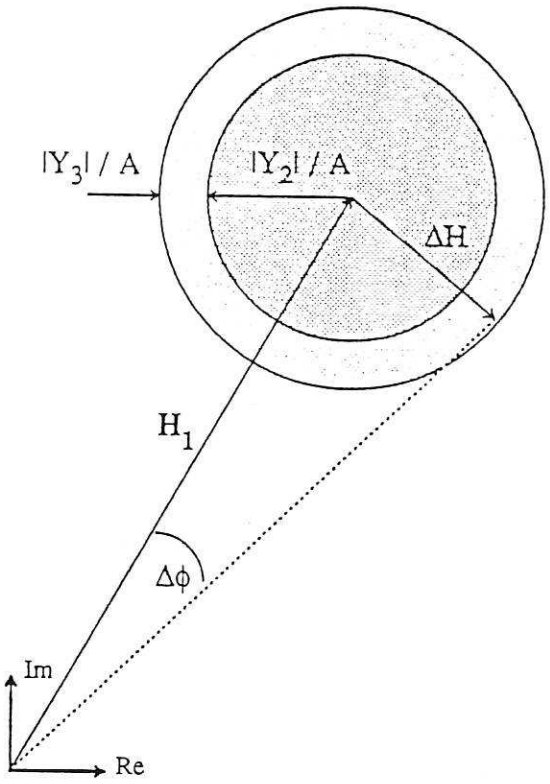

Fig 8 Worst case circles of uncertainty.

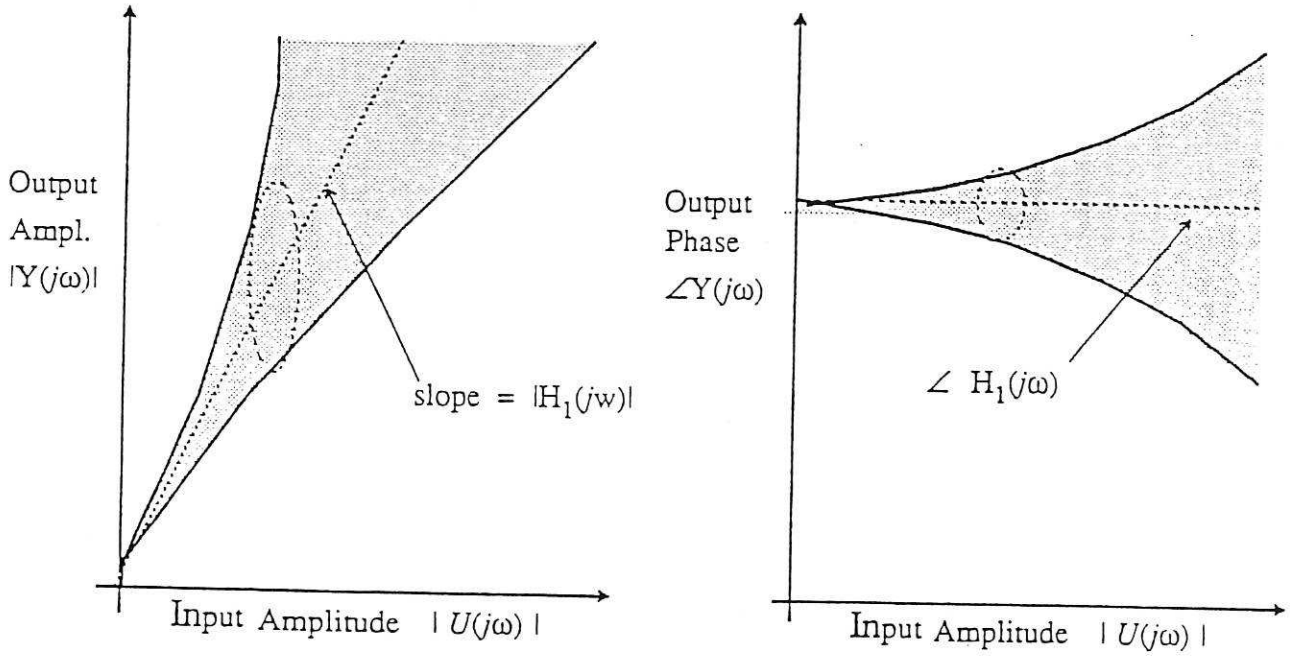

Fig 9 Worst case gain/phase response curves.

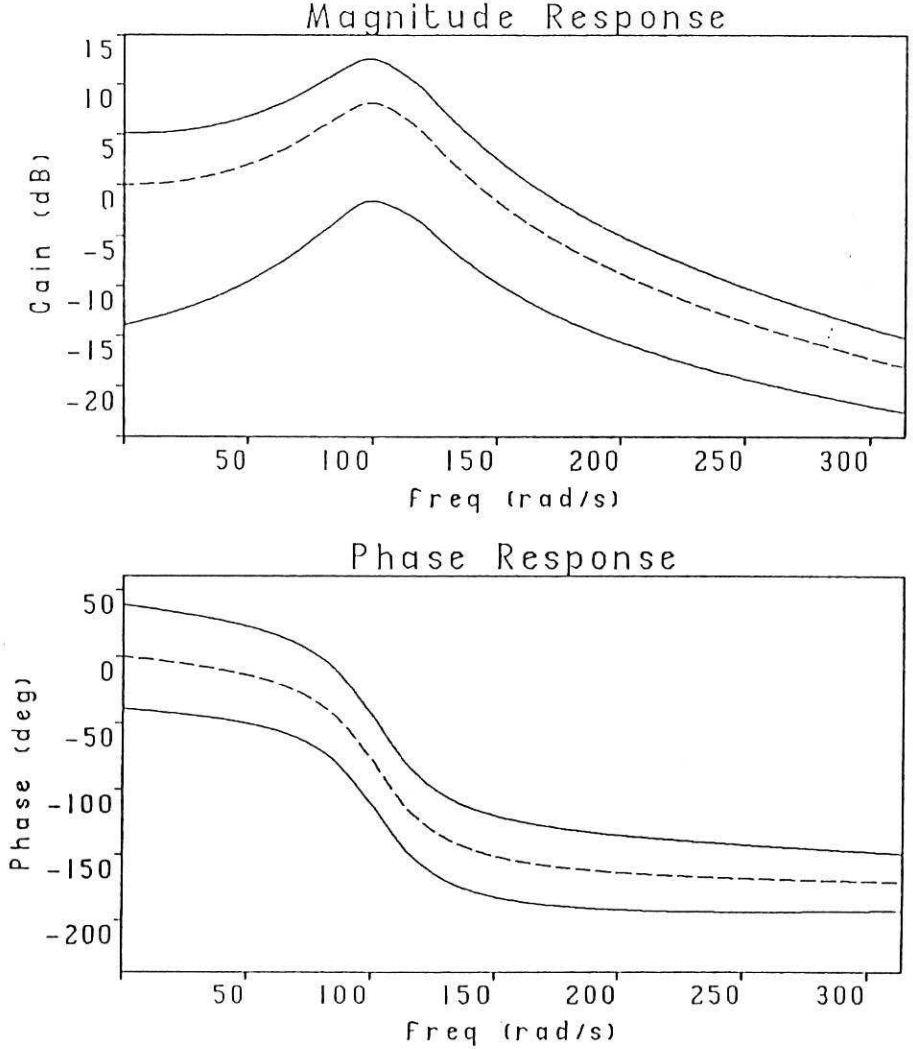

Fig 10 Worst case DF (A = 0.8).